Bulk viscosity due to kaons
in color-flavor-locked quark matter

Mark G. Alford and Matt Braby

Department of Physics

Washington University

St. Louis, MO 63130

USA

Sanjay Reddy

Theoretical Division

Los Alamos National Laboratory

Los Alamos, NM 87545

USA

Thomas Schäfer

Physics Department

North Carolina State University

Raleigh, NC 27695

USA

Abstract

We calculate the bulk viscosity of color-superconducting quark matter in the color-flavor-locked (CFL) phase. We assume that the lightest bosons are the superfluid mode H and the kaons K^0 and K^+, and that there is no kaon condensate. We calculate the rate of strangeness-equilibrating processes that convert kaons into superfluid modes, and the resultant bulk viscosity. We find that for oscillations with a timescale of milliseconds, at temperatures $T \ll 1$ MeV, the CFL bulk viscosity is much less than that of unpaired quark matter, but at higher temperatures the bulk viscosity of CFL matter can become larger.

1 Introduction

In this paper we calculate the bulk viscosity of matter at high baryon-number density (well above nuclear density) and low temperature (of order 10 MeV). On theoretical grounds it is expected that, at sufficiently high baryon-number density, three-flavor matter will be accurately described as a degenerate Fermi liquid of weakly-interacting quarks, with Cooper pairing at the Fermi surface (color superconductivity [1]) in the color-flavor-locked (CFL) channel [2]. That is the phase that we will study—the phase diagram at lower densities remains uncertain. The motivation for this calculation is that in nature the highest baryon-number densities are attained in the cores of compact stars, and it is speculated that quark matter, perhaps in the CFL phase, may occur there. This means that our best chance of learning about the high-density region of the phase diagram of matter is to make some connection between the physical properties of the various postulated phases of dense matter and the observable behavior of compact stars. Calculating the bulk viscosity of CFL quark matter is part of that enterprise.

Current observations of compact stars are able to give us measurements of quantities such as the mass, approximate size, temperature, spin and spin-down rate of these objects. These estimates are steadily improving, and other quantities, such as X-ray emission spectra, are becoming available. However, it is a challenge to connect these distantly-observable features to properties of the inner core of the star, where quark matter is most likely to occur (for reviews, see Ref. [3, 4]).

One possible connection is via oscillations of the compact star, which on the one hand are affected by the transport properties of the interior, and on the other hand may have observable effects on the behavior of the star. The bulk viscosity is one of the relevant transport properties, and is expected to play an important role in suppressing both vibrational and rotational oscillations. One particularly interesting application involves r-modes [5, 6, 7, 8]. If the viscosity of the star is too low, unstable r-mode bulk flows will take place, which quickly spin the star down, removing its angular momentum as gravitational radiation. The fact that we see quickly-spinning compact stars (millisecond pulsars) puts limits on the internal viscosity. If we can calculate the viscosity of the various phases of quark matter then the observations can be used to rule out some of those phases. There are various complications to this simple picture. Viscosity is very temperature-dependent, so to obtain useful limits we need good measurements of the temperatures of these stars. There are also some uncertainties about additional sources of damping that could help to quash r-modes. But the essential point is that viscosity calculations of the various phases are of great potential phenomenological importance, and in this paper we report on the results of such a calculation.

The phase that we choose to study is the CFL phase of quark matter. (The bulk viscosity for unpaired, non-interacting quark matter has been calculated previously [9, 10].) It is known that the mass of the strange quark induces a stress on the CFL phase that may lead to neutral kaon condensation [11, 12], producing a "CFL-K^0" phase. It is not known whether such condensation occurs at phenomenologically interesting densities, because of large uncertainties about instanton effects [13], and in this paper we will assume that kaon condensation has not occurred: our results are only applicable to the CFL phase, where there is a thermal population of K^0 and other mesons, but no condensation.

Bulk viscosity arises from a lag in the response of the system to an externally-imposed compression-rarefaction cycle. If there are some degrees of freedom that equilibrate on the same timescale as the period of the cycle, then the response will be out of phase with the applied compression, and work will be done. For astrophysical applications, such as r-modes of compact stars, we are interested in periods of order 1 ms, which is very long compared to typical timescales for particle interactions. In quark matter there is an obvious example of a suitably slowly-equilibrating quantity: flavor. Flavor is conserved by the strong and electromagnetic interactions, and only equilibrates via weak interactions.

In unpaired quark matter, the lightest degrees of freedom are the quark excitations around the Fermi surface, and their flavor-changing weak interactions produce a bulk viscosity [9]. However, in the CFL phase the quark excitations are gapped and their contribution to thermodynamic and transport properties at temperatures below the gap is irrelevant. Ignoring the quarks, then, the lightest degrees of freedom in CFL quark matter are the massless superfluid "H" modes, the electrons and neutrinos, the (rotated) photon, and the kaons. Of these, only the kaons carry flavor, so this paper will focus on the their contribution to flavor equilibration. In order to calculate the bulk viscosity of CFL matter at long timescales such as 1 ms we must therefore calculate the production and decay rates of thermal kaons. We expect the dominant modes to be ones that involve the H, like $K^0 \leftrightarrow H\,H$, and ones that involve the leptons, like $K^\pm \leftrightarrow e^\pm\,\nu$.

This paper is laid out as follows. Section 2 describes how the bulk viscosity is related to the production and decay rates of the kaons. Section 3 describes the basic thermodynamics of the system including the kaons and superfluid modes. Section 4 describes the overall calculation of the rates of the involved processes. Section 5 presents the results and conclusions.

2 Relating bulk viscosity to microscopic processes

The bulk viscosity is given by [9]

$$\zeta = \frac{2\bar{V}^2}{\omega^2(\delta V)^2}\frac{dE}{dt} \ , \tag{2.1}$$

where the system is being driven through a small-amplitude compression-rarefaction cycle with volume amplitude δV (see (2.3) below) and the driving angular frequency is ω. The average power dissipated per unit volume is

$$\frac{dE}{dt} = -\frac{1}{\tau\bar{V}}\int_0^\tau p(t)\frac{dV}{dt}dt \ , \tag{2.2}$$

where $\tau = 2\pi/\omega$. We can parameterize the volume oscillation by an amplitude $\delta V \ll \bar{V}$ (chosen to be real by convention), and the resultant pressure oscillation $p(t)$ by a complex amplitude δp which determines its strength and phase:

$$\begin{aligned}
V(t) &= \bar{V} + \mathrm{Re}(\delta V\,e^{i\omega t}) \\
p(t) &= \bar{p} + \mathrm{Re}(\delta p\,e^{i\omega t})
\end{aligned} \tag{2.3}$$

Substituting these into (2.2) and (2.1), we find that

$$\begin{aligned}
\frac{dE}{dt} &= -\frac{1}{2}\omega\,\text{Im}(\delta p)\,\frac{\delta V}{\bar{V}} \\
\zeta &= -\frac{\text{Im}(\delta p)}{\delta V}\frac{\bar{V}}{\omega}
\end{aligned}$$

(2.4)

We therefore expect that $\text{Im}(\delta p)$ will turn out to be negative. To determine this quantity, we note that the pressure is a function of the temperature and the chemical potentials. We assume that heat arising from dissipation is conducted away quickly, so the whole calculation is performed at constant T, and in order to find δp we only need to know how the chemical potentials vary in response to the driving oscillation. We expect the bulk viscosity to be most strongly influenced by the lightest excitations that carry flavor, and for the sake of definiteness we will take those to be kaons. Our analysis could easily be modified to treat the case where the lightest bosons were pions. At this point we do not have to specify whether our kaons are K^0 or K^+. The relevant chemical potentials are $\mu_d - \mu_s$ for the K^0 and $\mu_u - \mu_s$ for the K^+. For the following generic analysis we will just write the equilibrating chemical potential as "μ_K".

In thermal equilibrium, the distribution of kaons is determined by their dispersion relations (3.13) and the Bose-Einstein distribution. When the kaon population goes slightly out of equilibrium in response to the applied perturbation, strong interaction processes are still proceeding quickly: only weak interactions are failing to keep up. This means that we can always characterize our kaon population by the flavor chemical potential μ_K, so the kaon distribution has the form $n_K(p) \propto p^2/(\exp((E_K(p)-\mu_K)/T) - 1)$ (see Eq. (3.16)), and nonzero μ_K indicates deviation from equilibrium.

We express the variations in the chemical potentials for quark number and strangeness in terms of complex amplitudes $\delta\mu$, and $\delta\mu_K$,

$$\begin{aligned}
\mu(t) &= \bar{\mu} + \text{Re}(\delta\mu\,e^{i\omega t})\,, \\
\mu_K(t) &= \text{Re}(\delta\mu_K e^{i\omega t})\,.
\end{aligned}$$

(2.5)

Note that the term $-m_s^2/(2\mu)$ which is often described as an "effective chemical potential" is already included in the kaon dispersion relation (3.13), so in equilibrium, μ_K is zero. The pressure amplitude is then

$$\delta p = \left.\frac{\partial p}{\partial\mu}\right|_{\mu_K}\delta\mu + \left.\frac{\partial p}{\partial\mu_K}\right|_{\mu}\delta\mu_K = n_q\delta\mu + n_K\delta\mu_K\,,$$

(2.6)

(From now on all partial derivatives with respect to μ will be assumed to be at constant μ_K, and vice versa.) In principle one might worry that what we have called "n_K" is really $n_d - n_s$ (or $n_u - n_s$), but at temperatures below the gap, and in the absence of kaon condensation, thermal kaons make the dominant contribution to $n_d - n_s$ and $n_u - n_s$. From (2.6) and (2.4) we find

$$\zeta = -\frac{1}{\omega}\frac{\bar{V}}{\delta V}\left(\bar{n}_q\text{Im}(\delta\mu) + \bar{n}_K\text{Im}(\delta\mu_K)\right)\,.$$

(2.7)

3

To obtain the imaginary parts of the chemical potential amplitudes, we write down the rate of change of the corresponding conserved quantities,

$$
\begin{aligned}
\frac{dn_q}{dt} &= \frac{\partial n_q}{\partial \mu}\frac{d\mu}{dt} + \frac{\partial n_q}{\partial \mu_K}\frac{d\mu_K}{dt} &= -\frac{n_q}{\bar{V}}\frac{dV}{dt} \ , \\
\frac{dn_K}{dt} &= \frac{\partial n_K}{\partial \mu}\frac{\partial \mu}{dt} + \frac{\partial n_K}{\partial \mu_K}\frac{d\mu_K}{dt} &= -\frac{n_K}{\bar{V}}\frac{dV}{dt} - \Gamma_{\text{total}} \ .
\end{aligned}
\tag{2.8}
$$

All the partial derivatives are evaluated at equilibrium, $\mu = \bar{\mu}$ and $\mu_K = 0$. The right hand term on the first line expresses the fact that quark number is conserved, so when a volume is compressed, the quark density rises. On the second line, which gives the rate of change of kaon number, there is such a term from the compression of the existing kaon population, but there is also a net kaon annihilation rate of Γ_{total} kaons per unit volume per unit time, which reflects the fact that weak interactions will push the kaon density towards its equilibrium value. The annihilation rate will be calculated from the microscopic physics in section 4. For small deviations from equilibrium we expect Γ_{total} to be linear in μ_K, so it is convenient to write the rate in terms of an average kaon width γ_K, which is defined in terms of the total rate by writing

$$
\Gamma_{\text{total}} = \gamma_K \frac{\partial n_K}{\partial \mu_K}\delta\mu_K e^{i\omega t}
\tag{2.9}
$$

where the derivatives are evaluated at $\mu_K = 0$.

We now substitute the assumed oscillations (2.3) and (2.5) in to (2.8), and solve to obtain the amplitudes $\delta\mu$ and $\delta\mu_K$ in terms of the amplitude δV and angular frequency ω of the driving oscillation. Inserting their imaginary parts in (2.7) we obtain the bulk viscosity

$$
\zeta = C\frac{\gamma_{\text{eff}}}{\omega^2 + \gamma_{\text{eff}}^2}
\tag{2.10}
$$

where

$$
\gamma_{\text{eff}} = \gamma_K \left(1 - \frac{\left(\frac{\partial n_K}{\partial \mu}\right)^2}{\frac{\partial n_q}{\partial \mu}\frac{\partial n_K}{\partial \mu_K}}\right)^{-1} \approx \gamma_K
$$

$$
C = \left(\frac{\partial n_q}{\partial \mu}\right)^{-1}\frac{\left(\bar{n}_K\frac{\partial n_q}{\partial \mu} - \bar{n}_q\frac{\partial n_K}{\partial \mu}\right)^2}{\frac{\partial n_K}{\partial \mu_K}\frac{\partial n_q}{\partial \mu} - \left(\frac{\partial n_K}{\partial \mu}\right)^2} \approx \left(\frac{\partial n_K}{\partial \mu_K}\right)^{-1}\left(\bar{n}_K - \bar{n}_q\frac{\partial n_K}{\partial \mu}\left(\frac{\partial n_q}{\partial \mu}\right)^{-1}\right)^2
$$

$$
\tag{2.11}
$$

The approximate forms on the right hand side are valid for $T \ll \mu$. They follow from the fact that all the derivatives of the kaon free energy go to zero as $T \to 0$, so n_K and its derivatives are suppressed relative to $\bar{n}_q$ and $\partial n_q/\partial\mu$, which are of order μ^3 and μ^2 respectively.

To evaluate C and γ_{eff} we need the particle densities and their derivatives, which follow from the full free energy of the system, $\Omega = \Omega_{\text{CFL}-\text{quarks}}(\mu) + \Omega_K(\mu, \mu_K)$, where

4

$\Omega_{\text{CFL-quarks}}$ is the CFL quark free energy at zero temperature [14] and Ω_K is the kaon free energy (3.16). Then n_q and $dn_q/d\mu$ come dominantly from $\Omega_{\text{CFL-quarks}}$, and all the other quantities in (2.11) come from Ω_K. We can then see that the kaon free energy depends on $E_K(p) - \mu_K$, and we choose m_K to be independent of μ, so from the kaon dispersion relation (3.13) we see that the kaon free energy is a function of $\mu_K + m_s^2/(2\mu)$. This means that

$$\frac{\partial n_K}{\partial \mu} = -\frac{m_s^2}{2\mu^2} \frac{\partial n_K}{\partial \mu_K} \tag{2.12}$$

so terms in (2.11) involving $dn_K/d\mu$ are suppressed relative to those involving $dn_K/d\mu_K$.

From (2.10) we can already see how the bulk viscosity depends on the angular frequency ω of the oscillation and the equilibration rate γ_K. At fixed γ_K, the bulk viscosity decreases as the oscillation frequency rises; it is roughly constant for $\omega \lesssim \gamma_K$, and then drops off quickly as $1/\omega^2$ for $\omega \gg \gamma_K$. At fixed ω, the bulk viscosity is dominated by processes with rate $\gamma_K \sim \omega$, and their contribution is proportional to $1/\gamma_K$. If we imagine varying the rate but keeping other quantities fixed (e.g. by varying the coupling constant of the equilibrating interaction), then for $\gamma_K \ll \omega$ or $\gamma_K \gg \omega$ the bulk viscosity tends to zero. Thus very fast processes, such as strong interactions, are not an important source of bulk viscosity. The limit of zero equilibration rate *and* zero frequency is singular, and depends on the order of limits.

In this paper we will also be concerned with the temperature dependence of the bulk viscosity. This cannot be straightforwardly read off from (2.10) because the rates and particle densities depend on the temperature in complicated ways; however we expect that as we go to higher temperatures ($T \gg m_K, \mu_K$) the bulk viscosity will grow because the kaon density is rapidly increasing. In the limit of low temperature we expect the viscosity to be suppressed by $\exp((-m_K + \mu_K^{\text{eff}})/T)$ as the thermal kaon population disappears.

3 Dynamics of the light modes

In this section we lay out the properties of the lightest modes of the system, since they will dominate the transport properties. There is an exactly massless scalar Goldstone boson associated with spontaneous breaking of baryon number, and some light pseudoscalars associated with the spontaneous breaking of the chiral symmetry. We will ignore the η' mode associated with the breaking of $U(1)_A$, since $U(1)_A$ is explicitly broken in QCD at moderate densities.

3.1 The superfluid "H" mode

The CFL quark condensate breaks the exact $U(1)_B$ baryon number symmetry of the QCD Lagrangian, creating a superfluid with an exactly massless Goldstone boson H. The Lagrangian for the superfluid mode of the CFL phase is [15]

$$L_{\text{eff}} = \frac{N_c N_f}{12\pi^2} \Big[(\partial_0 \phi - \mu)^2 - (\partial_i \phi)^2 \Big]^2 \tag{3.1}$$

This Lagrangian is correct to leading (zeroth) order in α_s and to leading order in the derivatives of the ϕ field. This can be rescaled to give a conventionally normalized

kinetic term, and the total time-derivative term can be dropped [16], giving

$$L_{\text{eff}} = \tfrac{1}{2}(\partial_0\phi)^2 - \tfrac{1}{6}(\partial_i\phi)^2 - \frac{\pi}{9\mu^2}\partial_0\phi(\partial_\mu\phi)^2 + \frac{\pi^2}{108\mu^4}(\partial_\mu\phi\partial^\mu\phi)^2 \tag{3.2}$$

Ignoring the interaction terms for the moment, the dispersion relation for the H particle is

$$E_H(p) = v_H\, p \tag{3.3}$$

where $v_H^2 = 1/3$ is the ratio of the spatial and temporal derivatives above. In thermal equilibrium at temperature T, the H bosons have free energy

$$\Omega_H = \frac{T}{2\pi^2}\int_0^\infty dk\, k^2 \ln(1 - \exp(-v_H k/T)) = -\frac{\pi^2}{90 v_H^3}T^4 \tag{3.4}$$

and number density

$$n_H = \int \frac{d^3k}{(2\pi)^3} \frac{1}{\exp(E_H/T) - 1} = \frac{\zeta(3)}{\pi^2 v_H^3}T^3 \ . \tag{3.5}$$

The cubic and higher-order terms allow a single H to decay into multiple H particles. For energies far below μ the dominant process is $H \to HH$ [16, 17], whose rate can be calculated by taking the imaginary part of the 1-loop H self energy. Higher order corrections to the self energy are ignored, both in Ref. [16] and in this paper. These corrections could be calculated by taking into account quantum mechanical interference, the Landau-Pomeranchuk-Migdal (LPM) effect. This should only introduce a difference of $O(1)$ in the coefficient of the self-energy but would not change the parametric result. The self energy is given by Eq. (3.7) in Ref. [16],

$$\Sigma_H(p_0, p) = -\frac{4\pi^2}{81\mu^4} \sum_{s_1,s_2=\pm} \int \frac{d^3k}{(2\pi)^3} F(p_0, p, k)\left(\frac{s_1 s_2}{4E_1 E_2}\frac{1 + f(s_1 E_1) + f(s_2 E_2)}{i\omega - s_1 E_1 - s_2 E_2}\right), \tag{3.6}$$

where

$$F(p_0, p, k) \equiv \left[p_0^2 - v^2 p^2 - 2vk(p_0 - vk)\right]^2, \tag{3.7}$$
$$f(E) \equiv 1/(e^{E/T} - 1), \qquad E_1 \equiv vk, \qquad E_2 \equiv v|\boldsymbol{p} - \boldsymbol{k}|.$$

Ref. [16] showed that the real part of this self-energy is parametrically smaller than the imaginary part, so we will only concern ourselves with the imaginary part, which we will call Π_H. There is no contribution to the imaginary part when $s_1 = s_2 = -1$ as there is no pole in the integral. One can also show that the two terms where the signs of s_1 and s_2 are opposite are identical. We can then rewrite this in a slightly simpler and more suggestive form that will be used in Section 4.

$$\Pi_H(p_0, p) = \frac{2\pi^3 p_0^2}{81\mu^4 v^4}\frac{1}{1 + f(p_0)} \int \frac{d^3k}{2k_0(2\pi)^3} F(p_0, p, k)G(p_0, p, k)\ ,$$

$$G(p_0, p, k) = (1 + f(E_1))\left(\frac{1 + f(E_2)}{E_2}\,\delta(p_0 - E_1 - E_2) + 2\,\frac{f(E_2)}{E_2}\,\delta(p_0 - E_1 + E_2)\right).$$
$$\tag{3.8}$$

The H propagator can then be written as follows

$$D_H(p_0, p) = \frac{1}{p_0^2 - v_H^2 p^2 + i\Pi_H(p_0, p)} \tag{3.9}$$

and we will use this expression in section 4. It will be useful in the calculation of the decay rates to have the H self-energy at momenta and energies close to mass shell $(p_0 = vp)$. The self-energy is discontinuous at this point so there are two values Π_H^+ and Π_H^- depending on whether p_0 tends to vp from above or below,

$$
\begin{aligned}
\Pi_H^+(p) &= \lim_{\varepsilon \to 0} \Pi_H(vp + \varepsilon, p) &= -\frac{\pi p}{81\mu^4 v} \frac{1}{1 + f(vp)} \int_0^p dk\, I(p, k) \;, \\
\Pi_H^-(p) &= \lim_{\varepsilon \to 0} \Pi_H(vp - \varepsilon, p) &= \frac{2\pi p}{81\mu^4 v} \frac{1}{1 + f(vp)} \int_p^\infty dk\, I(p, k) \;.
\end{aligned}
\tag{3.10}
$$

where $I(p, k) = k^2(p - k)^2(1 + f(vk))f(vk - vp)$. As $T \to 0$, $\Pi_H^+(p) \propto p^6/\mu^4$, and $\Pi_H^-(p) \to 0$.

3.2 Pions and Kaons

The CFL quark condensate breaks the approximate $SU(3)$ chiral symmetry of the QCD Lagrangian, creating eight light pseudoscalar pseudo-Goldstone mesons. This octet is just a high-density version of the pion/kaon octet. It is described by an effective theory [18, 19]

$$L_{\text{eff}} = \tfrac{1}{4} f_\pi^2 \text{Tr}\Big(\nabla_0 \Sigma \nabla_0 \Sigma^\dagger - v_\pi^2 \partial_i \Sigma \partial_i \Sigma^\dagger\Big) + \cdots \tag{3.11}$$

where $\Sigma = \exp(iP^a \lambda^a / f_\pi)$, and the normalization of the GellMann matrices is $\text{tr}(\lambda^a \lambda^b) = 2\delta^{ab}$, which yields a conventionally normalized kinetic term for the Goldstone boson fields P^a. At asymptotic densities, weak-coupling calculations give [19]

$$f_\pi^2 = \frac{21 - 8\log(2)}{18}\left(\frac{\mu^2}{2\pi^2}\right) \qquad v_\pi^2 = \frac{1}{3} \;. \tag{3.12}$$

When weak interactions have equilibrated, the pseudoscalars $P = \pi^\pm, K^\pm, K^0, \overline{K^0}$ have dispersion relations [19, 11]

$$E_P = -\mu_P^{\text{eff}} + \sqrt{v_\pi^2 p^2 + m_P^2} \;, \tag{3.13}$$

where

$$
\begin{aligned}
\mu_{\pi^\pm}^{\text{eff}} &= \pm\frac{m_d^2 - m_u^2}{2\mu} \;, \\
\mu_{K^\pm}^{\text{eff}} &= \pm\frac{m_s^2 - m_u^2}{2\mu} \;, \\
\mu_{K^0, \overline{K^0}}^{\text{eff}} &= \pm\frac{m_s^2 - m_d^2}{2\mu} \;.
\end{aligned}
\tag{3.14}
$$

Because $m_s \gg m_u, m_d$, the K^0 and K^+ are expected to have the smallest energy gap, and so we focus on their contribution to the bulk viscosity. We are interested in studying small departures from equilibrium, where each meson has an additional chemical

potential $\delta\mu_P$. It will turn out that the K^0 makes the dominant contribution, so only $\delta\mu_{K^0}$ is relevant (Sec. 4.1).

The expression for the bulk viscosity (2.10) contains terms of the form $\partial n_K/\partial\mu$, which take into account the fact that the meson distributions depend on the meson dispersion relations, which via (3.14) depend on the quark chemical potential. In this paper we treat the meson masses m_{K^0} etc as constants, but in perturbative calculations they also depend on μ and the CFL pairing gap Δ (see section 3.3).

In thermal equilibrium at temperature T and with chemical potential μ_P, the free energy and number density of a meson P is

$$\Omega_P = \frac{T}{2\pi^2} \int_0^\infty dk\, k^2 \ln(1 - \exp(-(E_P - \delta\mu_P)/T)) \tag{3.15}$$

$$n_P = -\frac{\partial\Omega_P}{\partial\mu_P} = \frac{1}{2\pi^2} \int_0^\infty dk\, k^2 \frac{1}{\exp((E_P - \delta\mu_P)/T) - 1} \tag{3.16}$$

When weak interactions have equilibrated $\delta\mu_P = 0$, but when weak interactions are out of equilibrium the mesons may have nonzero chemical potentials.

3.3 Pseudo-Goldstone-boson masses

Although we treat the masses as constants, they are predicted to have density dependence in high density QCD [13]

$$\begin{aligned}
m_{\pi^\pm}^2 &= \frac{1}{f_\pi^2}(2A + 4Bm_s)(m_u + m_d) \ , \\
m_{K^\pm}^2 &= \frac{1}{f_\pi^2}(2A + 4Bm_d)(m_u + m_s) \ , \\
m_{K^0,\overline{K^0}}^2 &= \frac{1}{f_\pi^2}(2A + 4Bm_u)(m_d + m_s) \ ,
\end{aligned} \tag{3.17}$$

where A is positive and related to instantons [20, 21]. In the limit of asymptotically large density the coefficient A can be computed reliably, but at moderate density its value is quite uncertain [13]. Asymptotic-density QCD calculations [19, 11] also yield

$$B = \frac{3\Delta^2}{4\pi^2} \ , \tag{3.18}$$

although it is not clear how well these expressions can be trusted at densities of phenomenological interest. We will assume that A and B are such that there is no meson condensation at zero temperature, which means that all the meson masses are greater than their effective chemical potentials.

3.4 Weak interactions between light bosons

We have argued above that the bulk viscosity will arise from flavor violation, which will be dominated by conversion between the lightest pseudo-Goldstone modes (neutral kaons, typically), which carry flavor, and the superfluid H modes, which are flavorless. The dominant effect of the weak interaction will be to introduce mixing between the

8

K^0 and the H, in the form of a $K^0 \leftrightarrow H$ vertex (3.26) in the effective theory. We now calculate the strength of that coupling.

The Lagrangian density for the H modes can be written in a nonlinear form analogous to (3.11) for the pseudoscalars, so the leading terms in the CFL effective theory become [18],

$$\mathcal{L}_{\text{eff}} = \frac{f_\pi^2}{4}\text{Tr}\left[\nabla_0\Sigma\nabla_0\Sigma^\dagger - v_\pi^2\partial_i\Sigma\partial_i\Sigma^\dagger\right] + 12f_H^2\left[\nabla_0 Z\nabla_0 Z^* - v_H^2\partial_i Z\partial_i Z^*\right] \qquad (3.19)$$

where $Z = \exp(iH/2\sqrt{6}f_H)$ is the field related to the breaking of $U(1)_B$ and f_H is the corresponding decay constant. At large density the coefficients of the CFL effective Lagrangian can be determined in perturbation theory. At leading order $v_\pi^2 = v_H^2 = 1/3$, f_π is given by (3.12), and from Ref. [19] we obtain

$$f_H^2 = \frac{3}{4}\left(\frac{\mu^2}{2\pi^2}\right) . \qquad (3.20)$$

Under an element $(L, R, \exp(i\alpha))$ of the the chiral flavor and baryon number symmetry group $SU(3)_L \times SU(3)_R \times U(1)_V$, the left-handed quarks, right-handed quarks, and bosons transform as follows:

$$\begin{aligned}
q_L &\rightarrow \exp(i\alpha)L\,q_L , \\
q_R &\rightarrow \exp(i\alpha)R\,q_R , \\
\Sigma &\rightarrow L\,\Sigma\,R^{-1} , \\
Z &\rightarrow \exp(i\alpha)\,Z .
\end{aligned} \qquad (3.21)$$

The weak Hamiltonian breaks the approximate flavor symmetry of QCD, and only acts on left-handed fields. The elementary process that is relevant to kaon decay is the conversion between strange quarks and down quarks via exchange of a $W^\pm$, which can be treated at energy scales well below 100 GeV as a four-fermion interaction (Ref. [22], sect. II-3 and II-4),

$$\mathcal{L}_{\text{weak}} = \frac{G_F V_{ud}V_{us}}{\sqrt{2}}(\overline{s}\gamma^\mu u)_L(\overline{u}\gamma_\mu d)_L + h.c. \qquad (3.22)$$

where $V_{ud}V_{us} \approx 0.215(3)$. In order to determine how this interaction is represented in the low energy effective theory of the CFL phase, we introduce the spurion field Λ_{ds} which transforms as $\Lambda_{ds} \rightarrow L\Lambda_{ds}L^\dagger$. In the QCD vacuum we set $\Lambda_{ds} = \lambda_6$ using the usual notation for the GellMann matrices (Ref. [22], sect. II-2), i.e. $(\Lambda_{ds})_{\alpha\beta} = \delta_{2\alpha}\delta_{3\beta} + \delta_{3\alpha}\delta_{2\beta}$. Thus each time this spurion field occurs in an interaction, it mediates a conversion of downness into strangeness, or vice versa. The lowest-order terms in the effective theory that involve such a conversion are obtained by writing down the lowest-order terms that contain Λ_{ds} and are invariant under spatial rotations and $SU(3)_L \times SU(3)_R \times U(1)_V$:

$$\mathcal{L}_{\text{weak}} = f_\pi^2 f_H^2 G_{ds}\text{Tr}\left[\Lambda_{ds}\left(\Sigma\partial_0\Sigma^\dagger\,Z\partial_0 Z^* - v_{ds}^4\Sigma\partial_i\Sigma^\dagger\,Z\partial_i Z^*\right)\right] \qquad (3.23)$$

where G_{ds} and v_{ds} are new couplings in the effective action.

Dimensional analysis suggests that $G_{ds} \sim G_F$ and $v_{ds} \sim 1$. If the density is large we can be more precise and determine the coupling constants using a simple matching
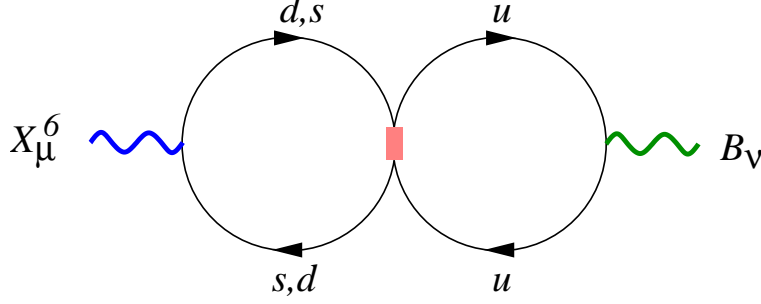
9

Figure 1: Leading contribution to the $X_\mu^6 B_\nu$ polarization function in the microscopic theory with gauged chiral and baryon number symmetries. The shaded bar corresponds to the vertex of (3.22), which is the low energy limit of a W-boson-mediated interaction.

argument. For this purpose we gauge the $SU(3)_L$ and $U(1)_B$ symmetries. We will denote the corresponding gauge fields X_μ^A and B_μ. The flavor-violating term (3.23) in the effective action leads to mixing between the X_μ^6 and B_μ gauge bosons. By matching to a calculation of the mixing term in the microscopic theory (3.22), we now proceed to determine G_{ds} in terms of G_F.

In the effective theory, the Σ field has one left-handed quark index so $\partial_\mu \Sigma \to (\partial_\mu + X_\mu^A \lambda_A)\Sigma$. For the superfluid mode, $\partial_\mu Z \to (\partial_\mu + B_\mu)Z$. Substituting into (3.23) and evaluating in the CFL vacuum ($\Sigma = 1$) we find the mixing term is

$$\mathcal{L}_{\text{mix}} = 2G_{ds}f_\pi^2 f_H^2(X_0^6 B_0 - v_{ds}^4 X_i^6 B_i) . \tag{3.24}$$

In the microscopic theory, the corresponding calculation is the computation of the $X_\mu^6 B_\nu$ polarization function. At weak coupling the dominant contribution comes from the two-loop diagram shown in Fig. 1. The evaluation of the Feynman diagram is described in Appendix A. The result (A.5) is

$$G_{ds} = \sqrt{2}V_{ud}V_{us}\,G_F \qquad v_{ds}^2 = v^2 = 1/3. \tag{3.25}$$

It is now straightforward to read off the $K^0 \to H$ amplitude. Linearizing (3.23), we find

$$\mathcal{L} = G_{ds}f_\pi f_H \left(\partial_0 K^0 \partial_0 H - v_{ds}^4 \partial_i K^0 \partial_i H\right) \tag{3.26}$$

with G_{ds} and v_{ds} given in (3.25). This leads to a vertex factor for the K-H interaction given by

$$A = G_{ds}f_\pi f_H(p_0^2 - v_{ds}^4\, p^2); \tag{3.27}$$

This is the value of the K^0-H vertex in Feynman diagrams such as Fig. 2. Combining this vertex factor and the Lagrangian for the H, we can calculate the matrix element for conversion between a kaon with 4-momentum p and two Hs with 4-momenta k and q,

$$M_{K^0HH}^2(p,k,q) = \frac{G_{ds}^2 f_\pi^2\,(p_0^2 - v_{ds}^4 p^2)^2}{144 f_H^2}\left(p_0(k \cdot q) + k_0(p \cdot q) + q_0(p \cdot k)\right)^2 |D_H(p_0,p)|^2 , \tag{3.28}$$

where D_H is the H-propagator (3.9).

10

Figure 2: The $K^0 \to H\,H$ diagram, including the $K^0 \to H$ vertex (square), a full H propagator (thick line) and the $H \to H\,H$ vertex (round). All external lines are amputated.

4 Rates of strangeness re-equilibration processes

4.1 Neutral Kaon Rates

In principle, the correct way to calculate the K^0 annihilation rate is as follows. As noted above, the weak interaction introduces a small mixing between the K^0 and the H. We rediagonalize the kinetic terms in the effective action, in terms of new fields E_K (which is the kaon with a tiny admixture of H) and E_H (which is the H with a tiny admixture of K^0). We have already seen that the H has a width, arising from the possibility of $H \to H\,H$[1]. When we diagonalize, this will induce a width for the E_K. Because the E_K is almost the same state as the kaon, the E_K width is a very good estimate of the K^0 width. In terms of the original basis, this width arises from the vertex shown in Fig. 2. In the interests of brevity, we do not rediagonalize, but simply calculate the contribution of the vertex shown in Fig. 2 to the kaon annihilation rate. This comes via the processes $K^0 \leftrightarrow H\,H$ and $H\,K^0 \leftrightarrow H$. The net kaon annihilation rate is

$$\Gamma_{\text{total}} = \Gamma_{\text{forward}} - \Gamma_{\text{backward}} = (1 - e^{-\delta\mu_{K^0}/T})\Gamma_{\text{forward}} \approx \frac{\delta\mu_{K^0}}{T}\Gamma_{\text{forward}}\ , \qquad (4.1)$$

where we have used the properties of the Bose-Einstein distributions. We keep only first order in $\delta\mu_{K^0}$, and obtain the average kaon width γ_K (2.9), remembering that $\delta\mu_K$ in section 2 was the amplitude of a complex oscillation, so $\delta\mu_{K^0} = \delta\mu_K \exp(i\omega t)$,

$$\gamma_K = \left(\frac{\partial n_K}{\partial \mu_K}\right)^{-1} \frac{\Gamma_{\text{forward}}(\delta\mu_K = 0)}{T}\ . \qquad (4.2)$$

We can therefore obtain the average kaon width simply from the forward rates $K^0 \to H\,H$ and $H\,K^0 \to H$. The contribution from $K^0 \to H\,H$ is

$$\Gamma_{K^0 \to HH} = \frac{1}{2} \int_p \int_{q_1} \int_{q_2} |M|^2 (2\pi)^3 \delta(\boldsymbol{p} - \boldsymbol{q_1} - \boldsymbol{q_2}) (2\pi)\delta(p_0 - vq_1 - vq_2)\, F_{BE}(p_0, q_1, q_2) \qquad (4.3)$$

with $|M|^2$ given in (3.28) and $F_{BE}(p_0, q_1, q_2) = f(p_0 - \delta\mu_{K^0})(1 + f(vq_1))(1 + f(vq_2))$. The rate for $K^0\,H \to H$ can be obtained by multiplying by 2 for the symmetry factor difference, switching $q_2 \to -q_2$ in both delta functions and turning $(1 + f_{vq_2}) \to f_{vq_2}$ to

---

[1]There are also decays involving three or more H particles, but we expect these to be suppressed, since the H is derivatively coupled, and the greater the number of H particles involved, the smaller the momentum carried by each of them.

make that H an incoming particle. Adding the two contributions, and performing the q_2 integral using the momentum-conserving delta-function, we obtain the total forward rate

$$\Gamma_{\text{forward}} = G_{ds}^2 f_\pi^2 f_H^2 \int_p f(E_K)\,(1 + f(E_K))\,\frac{(E_K^2 - v^4\,p^2)^2\,\Pi_H(E_K, p)}{(E_K^2 - v^2\,p^2)^2 + \Pi_H(E_K, p)^2} \qquad (4.4)$$
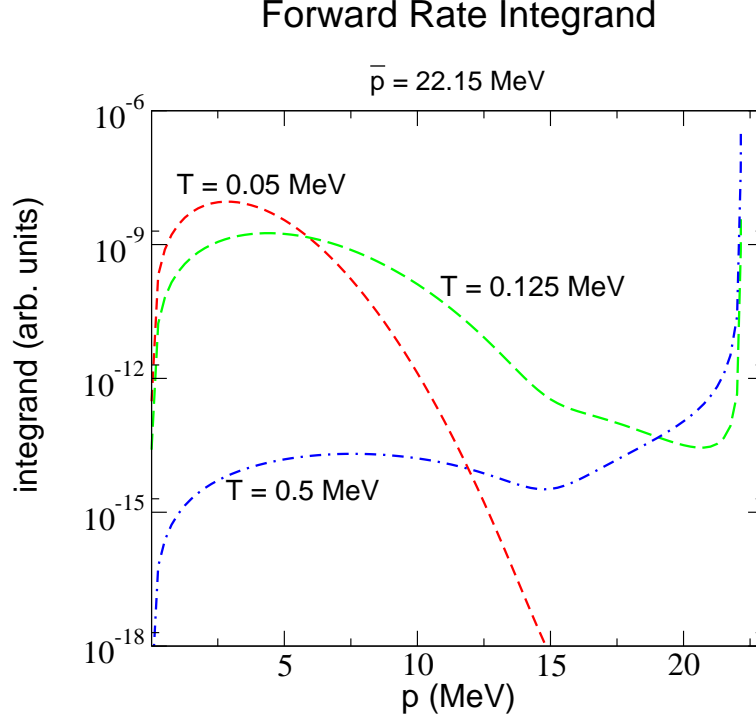
where $\Pi_H(E_K, p)$ was defined in Eq. (3.8).

Forward Rate Integrand

Figure 3: Plot of the integrand of (4.4) as a function of momentum for $p < \bar{p}$. In this plot $\mu = 400$ MeV, $m_s = 120$ MeV, and $m_K = 27.92$ MeV, so $\bar{p} = 22.15$ MeV and $T_a \sim 0.14$ MeV. For $T \ll \bar{p}$ the integral is dominated by low-momentum kaons, i.e. $p \ll \bar{p}$ ($T = 0.05$ MeV line in plot). But as T gets closer to $\bar{p}$, the near-singularity at $p = \bar{p}$ becomes more important, and at $T = 0.5$ MeV the integral is actually dominated by the region where p is very close to $\bar{p}$.

In general this can be evaluated numerically and then combined with (4.2),(2.10),(2.11) to obtain the bulk viscosity. However for certain temperatures, the integrand is dominated by momentum that make the denominator as small as possible, i.e. when $E_K = v\,p$. This corresponds to the $H \leftrightarrow K^0$ resonance, at which the kaon has a special momentum $\bar{p}$ such that an H with that momentum is also on shell,

$$\bar{p} = \frac{m_K^2 - \mu_{K^0}^{\text{eff}\,2}}{2\,v\,\mu_{K^0}^{\text{eff}}} = \frac{\delta m}{v}\left(1 + \frac{\delta m}{2\mu_{K^0}^{\text{eff}}}\right)\,. \qquad (4.5)$$

where $\delta m = m_K - \mu_{K^0}^{\text{eff}}$. Near this momentum, the virtual H in Fig. 2 is almost on shell, so momenta close to $\bar{p}$ dominate the integral. As long as the numerator is slowly

varying, we can approximate the sharp peak as a delta-function, obtaining

$$\Gamma_{\text{forward}} \approx \frac{G_{ds}^2 f_\pi^2 f_H^2}{18\sqrt{3}\pi} (1 + m_K^2/\mu_{K^0}^{\text{eff }2}) \bar{p}^4 \frac{e^{v\bar{p}/T}}{(e^{v\bar{p}/T}-1)^2} \; . \tag{4.6}$$

This expression becomes invalid at very low temperature $T \ll T_a$, when there are very few kaons with momentum $\bar{p}$ so the main contribution does not come from $p \approx \bar{p}$, and at very high temperature $T \gg T_b$ when there are so many thermal kaons with $p > \bar{p}$ that they outweigh the contribution from the resonance. One determines T_a and T_b by setting the non-resonant contribution equal to the resonant value from Eq. (4.6), giving $T_{a,b}$ as a function of δm. T_b has to be determined numerically and we found that $T_b \sim 9$ MeV for $\delta m = 0.1$ MeV and monotonically increases as δm increases, so T_b is almost always higher than the temperature range that is of physical interest. T_a is given by the following condition

$$T_a \approx \frac{\delta m^2}{2\mu_{K^0}^{\text{eff}}} \left(\ln\left(\frac{\mu^4}{\delta m \, (m_K \, T_a)^{3/2}}\right) \right)^{-1} \; , \tag{4.7}$$

where the T_a dependence on the right side is logarithmically weak, so we expect that $T_a \lesssim \delta m^2/(2\mu_{K^0}^{\text{eff}})$.

The integrand of (4.4) is plotted in Fig. 3, for several different values of the temperature, showing that for lower temperatures, $T < T_a$, the integrand is a smooth function, with a broad peak in the low-momentum region, but as the temperature rises, and the number of thermal kaon with momentum $\bar{p}$ rises, the integrand develops a very sharp peak at $p = \bar{p}$, where the intermediate H is on shell.

4.2 Charged Kaon Rates

In principle there is also a contribution to kaon number violation from the charged kaon modes, which necessarily involve charged leptons. We will now show that this can be neglected compared to the contribution from the neutral kaons. The lightest charged kaon is the K^+, and the relevant creation/annihilation reactions are

$$K^+ \leftrightarrow e^+ \nu_e \tag{4.8}$$

$$K^+ + e^- \leftrightarrow \nu_e \tag{4.9}$$

$$K^+ + \bar{\nu}_e \leftrightarrow e^+. \tag{4.10}$$

The matrix element for this process has been calculated in Ref. [23, 24] and is given by

$$A = G f_\pi \sin\theta_c p_\mu \bar{e}(k_1) \gamma^\mu (1 - \gamma_5) \nu(k_2), \tag{4.11}$$

where G is the appropriate coupling constant for the charged kaons in the medium, which we expect is of order G_F. Summing over initial spins and averaging over final spins, we find

$$M^2 = G^2 f_\pi^2 \sin^2\theta_c \, m_e^2 \, (k_1 \cdot k_2) \tag{4.12}$$

13

The rate of the first reaction is

$$\Gamma = \int_0^{x0} dx \int_{y_1}^{y_2} dy\, x\, y\, \frac{x + y + \mu_{K^+}^{\text{eff}}/T}{x + y}(1 - z)F(x, y) \tag{4.13}$$

$$z = \frac{1}{2v^2 xy}\left((x^2 + y^2)(1 - v^2) + 2(x + y)\mu_{K^+}^{\text{eff}}/T + 2xy + (\mu_{K^+}^{\text{eff}\,2} - m_{K^+}^2)/T^2\right)$$

$$F(x, y) = \frac{\delta\mu_{K^+}}{T}\frac{e^{x+y}}{(e^{x+y} - 1)(e^x + 1)(e^y + 1)}.$$

where $F(x, y)$ is the product of the distribution functions for the kaon and two leptons to lowest order in $\delta\mu_{K^+}$. The rates for the second and third reactions, which are identical for a massless electron, can be derived from a simple change of $x \to -x$ and $y \to -y$, respectively. They can then be evaluated numerically. Note that these calculations are done keeping only the lowest order term in m_e and setting $\mu_e = 0$.

We can then compare this rate to the rate for neutral kaon decay and find that

$$\frac{\Gamma_{K^+}}{\Gamma_{K^0}} \sim \frac{T^2}{\mu^2}, \tag{4.14}$$

for $m_{K^0} \approx m_{K^+}$, so the contribution from charged kaons is suppressed by a factor of $(T/\mu)^2$. This is to be expected, since the phase space for quarks is of order $\mu^2 T$, localized near the quark Fermi surface, whereas the phase space for electrons is of order T^3, since in the CFL phase there is no Fermi sea of electrons.

5 Results

Our result for contribution of kaons to the bulk viscosity of CFL quark matter is given by equations (2.10), (2.11), (4.2), (4.4). The bulk viscosity is most sensitive to the temperature, and to the kaon energy gap

$$\delta m \equiv m_K - \mu_{K^0}^{\text{eff}} = m_K - \frac{m_s^2 - m_d^2}{2\mu} . \tag{5.1}$$

It also depends on the orthogonal combination $m_K + \mu_{K^0}^{\text{eff}}$, the quark chemical potential μ and CFL pairing gap Δ. As discussed in section 3.3, we have no reliable way to calculate m_K in the density range of interest for compact stars, so in presenting our results we will treat δm and T as parameters.

Using the definitions of the densities of kaons and quarks, one can derive the asymptotic versions of C for temperatures far above and far below the kaon energy gap (Table 1). One can also derive the low temperature version of the rate and from that, combined with C, we can get the low temperature version of the bulk viscosity (Table 2). As one would expect, most kaon-related quantities, including the bulk viscosity, are suppressed by $\exp(-\delta m/T)$ at low temperatures. This is because the energy gap δm is the minimum energy required to create a K^0, so the population of thermal kaons is suppressed by a Boltzmann factor.

To illustrate the likely contribution of kaons to the bulk viscosity of quark matter in compact stars, we now evaluate the bulk viscosity numerically for a range of δm and T.

quantity	asymptotic form	
	$T \ll \delta m$	$m_K \ll T \ll \mu$
n_K	$(m_K T)^{3/2} e^{-\delta m/T}$	T^3
$\frac{\partial n_K}{\partial \mu^{\mathrm{eff}}_{K^0}}$	$m_K (m_K T)^{1/2} e^{-\delta m/T}$	T^2
$\frac{\partial n_K}{\partial \mu}$	$-\frac{m_K^2}{\mu}(m_K T)^{1/2} e^{-\delta m/T}$	$-\frac{m_K}{\mu} T^2$
n_q	μ^3	μ^3
$\frac{\partial n_q}{\partial \mu}$	μ^2	μ^2
C	$m_K^3 (m_K T)^{1/2} e^{-\delta m/T}$	T^4

Table 1: Asymptotic forms for the densities and the C parameter. Constant numerical factors are not shown and it is implicitly assumed that $T < 0.57\Delta$ so that there is a CFL condensate, even when $T \gg m_K$.

quantity	approximate form	
	$T < T_a(\delta m) \ll \delta m$	$T_a(\delta m) < T \lesssim \delta m$
$\Gamma_{\mathrm{forward}}$	$G_F^2 \sqrt{m_K^3 T^3}\, \delta m^5\, e^{-\delta m/T}$	$G_F^2\, \mu^4\, \bar{p}^4\, e^{-v\bar{p}/T}$
γ_{eff}	$G_F^2\, \delta m^5$	$G_F^2\, \mu^4\, \bar{p}^4\, (m_K T)^{-3/2}\, e^{-\delta m^2/(2\,\mu^{\mathrm{eff}}_{K^0})\, T}$
ζ	$G_F^2\, \delta m^5\, m_K^{7/2} T^{1/2}\, e^{-\delta m/T}\, \omega^{-2}$	$G_F^2\, \mu^4 \bar{p}^4\, m_K^2\, T^{-1}\, e^{-v\bar{p}/T}/(\gamma_{\mathrm{eff}}^2 + \omega^2)$

Table 2: Approximate forms of the bulk viscosity and related quantities, for small T. Constant numerical factors are not shown. The rate has two separate ranges within the $T \ll \delta m$ region: $T < T_a \ll \delta m$ and $T_a < T \ll \delta m$, where $T_a \lesssim \delta m^2/(2\,\mu^{\mathrm{eff}}_{K^0})$ (4.7). Note that $\bar{p}$ is related to δm by (4.5). The low temperature entry for ζ is in general proportional to $(\gamma_{\mathrm{eff}}^2 + \omega^2)^{-1}$ rather than just ω^{-2}, but in this temperature range γ_{eff} is always much less than astrophysically relevant frequencies ($\omega \gtrsim 1$ Hz). There is no third column for the higher end of the range of temperatures that we study in this paper, $T \sim m_K, \mu^{\mathrm{eff}}_{K^0}$, because although we can still use (4.6) for $\Gamma_{\mathrm{forward}}$, there is no simple form for $\frac{\partial n_K}{\partial \mu^{\mathrm{eff}}_{K^0}}$ and hence for γ_{eff} or ζ.

Our calculations are performed at $\mu = 400$ MeV. We vary δm by varying m_K with $\mu_{K^0}^{\text{eff}}$ fixed at 17.92 MeV, corresponding to $m_s = 120$ MeV.

Compact stars have internal temperatures in the MeV range immediately after the supernova, and then cool to temperatures in the keV range over millennia, so we explore the range 0.01 MeV $\lesssim T \lesssim 10$ MeV. Since m_K and $\mu_{K^0}^{\text{eff}}$ are both expected to be of order tens of MeV [13], we expect δm to be generically of the same order, so we explore the range 0.1 MeV $\lesssim \delta m \lesssim 10$ MeV.

The bulk viscosity is determined by the kaon equilibration rate γ_K (4.2) and the coefficient C (2.11), so we plot these quantities separately before plotting the bulk viscosity.

5.1 Proportionality constant C (Fig. 4)
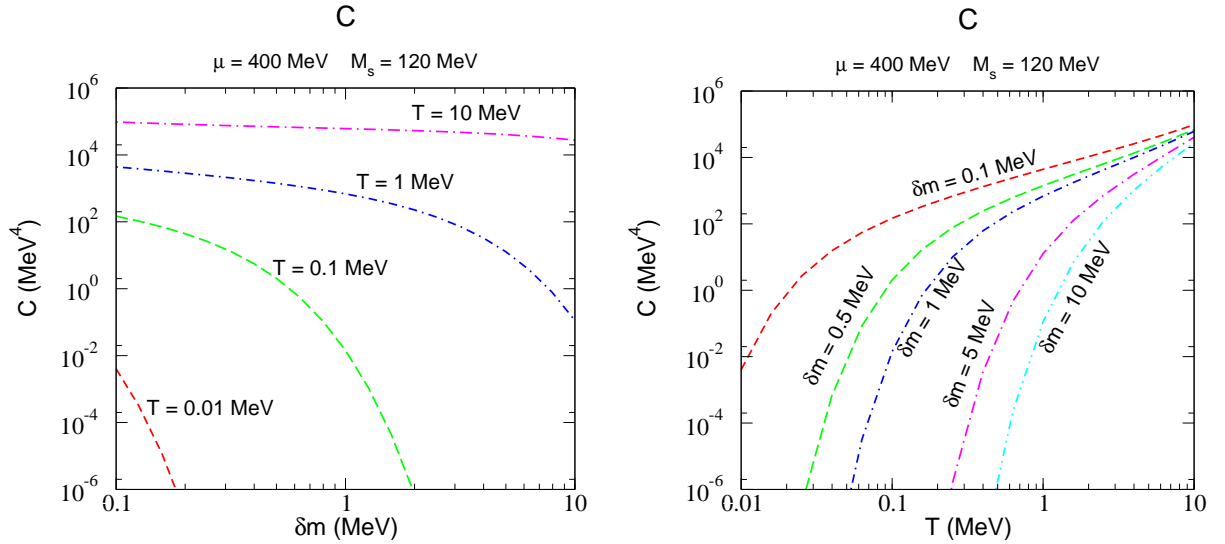
Figure 4: Coefficient C (2.11) as a function of δm (left panel) and temperature (right panel)

In Fig. 4 we show how C depends on δm and T. Roughly speaking, C measures how sensitive the kaon and quark number are to changes in μ_K and μ. At low temperatures $T \ll \delta m$, C is suppressed by an exponential factor $\exp(-\delta m/T)$, so the curves drop rapidly in the high δm region of the left panel, and the low T region of the right panel. We also see that the curves for different δm start to converge at high temperature (right panel). This is because at high enough temperature (beyond the range that we study) C would become proportional to T^4, independent of δm (see table 1).

5.2 Kaon width γ_{eff} (Fig. 5)

In Fig. 5 we show how the neutral kaon effective width γ_K depends on T and δm. (We also show one charged kaon width curve to illustrate that it is subleading (4.14)).

The δm-dependence is shown in the left panel. From Table 2, we expect that at a fixed temperature T, for sufficiently large δm, $T_a(\delta m)$ will become greater than T,
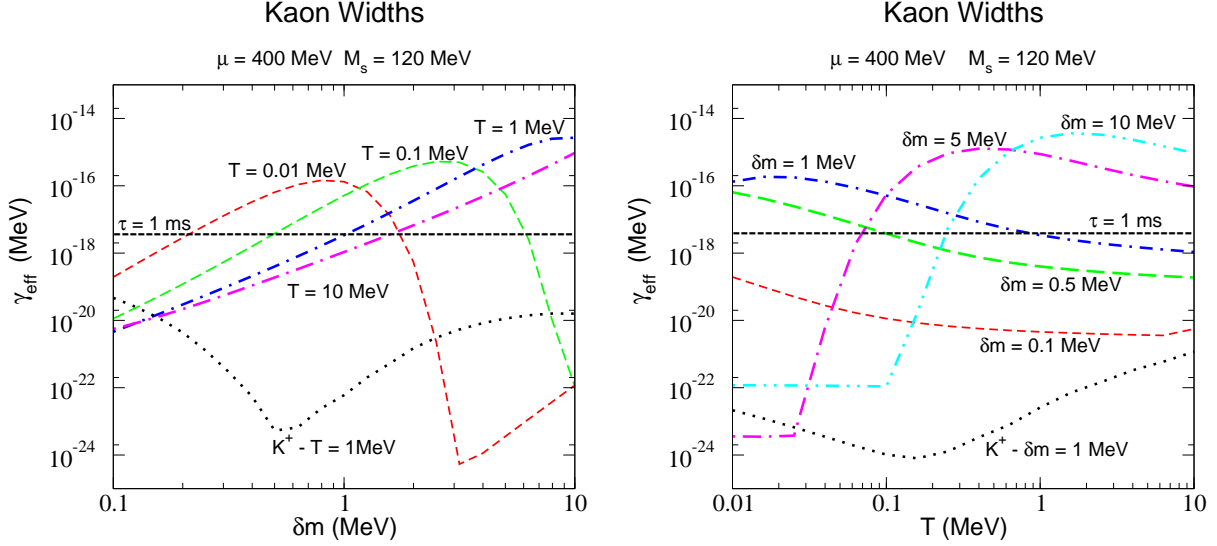
Figure 5: Plot of average K^0 decay width γ_K (4.2), (4.4) as a function of δm (left panel) and temperature (right panel). The horizontal dashed line shows where the width is 1 kHz ($\omega/2\pi = 1$ ms^{-1}), the fastest rotation rate of compact stars. The charged kaon width is also shown (dotted line) to illustrate that it is a subleading contribution to strangeness equilibration (4.14). The transition that occurs at $\delta m \approx T$ is where the rate becomes dominated by the H resonance (Section 4.1).

and γ_K will then rise as δm^5. This is seen at the upper end of the $T = 0.01$ MeV curve, and corresponds to the region where low-momentum ($p < \bar{p}$) kaons dominate the rate. For the rest of the $T = 0.01$ MeV curve, and for all the other curves in the plot, the equilibration is dominated by kaons at the H-resonance, with momentum $\bar{p}$. The width shows a peak as a function of δm, which follows from the approximate form for γ_{eff} given in table 2 (second column). Using (4.5) to relate δm to $\bar{p}$, one can see $\gamma_{\mathrm{eff}} \sim \delta m^4 \exp(-\delta m^2/(2\mu_{K^0}^{\mathrm{eff}}T))$, which is peaked at $\delta m_{\mathrm{peak}} = 2\sqrt{\mu_{K^0}^{\mathrm{eff}}T}$. For our plots $\mu_{K^0}^{\mathrm{eff}} \approx 30$ MeV, which gives the observed positions of the peaks.

The T-dependence is shown in the right panel. At the very lowest temperatures γ_{eff} will have a constant value which depends on δm (Table 2). This is clear in the curves for $\delta m = 5$ MeV and $\delta m = 1$ MeV. As with the large δm region of the left panel, this is where the low momentum kaons are dominating the rate. In the intermediate temperature region the width rises quickly and then peaks and drops off slowly. This comes from competition (4.2) between $\Gamma_{\mathrm{forward}}/T$, which is monotonically increasing with T (4.6), and $(dn_K/d\mu_K)^{-1}$, which is monotonically decreasing with T. At high enough temperature, The expression (4.6) for $\Gamma_{\mathrm{forward}}/T$ rises as T, while $dn_K/d\mu_K$ rises more quickly, so the width drops.

At high enough T, the curve with $\delta m = 0.1$ MeV starts to bend upwards. This feature actually corresponds to $T \gtrsim T_b$ (from Section 4.1) where (4.6) becomes invalid and kaons with high momentum ($p > \bar{p}$) dominate the rate. For the other curves, T_b is beyond the range that we study.
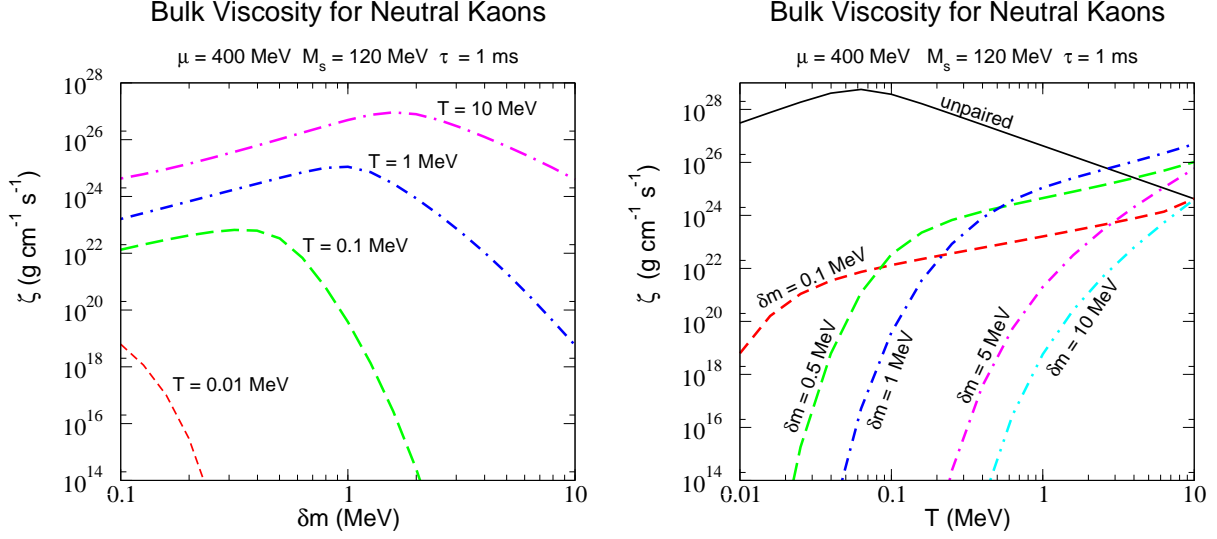
17

5.3   Bulk viscosity ζ (Fig. 6 and 7)

Figure 6: Plot of bulk viscosity as a function of δm (left panel) and temperature (right panel).

It is useful to compare the behavior of the bulk viscosity in CFL quark matter with its behavior in quark matter phases whose re-equilibration is dominated by ungapped fermionic modes such as the 2SC or single-flavor phases (see solid black line in Fig. 6). In such phases, the bulk viscosity shows a peak as a function of T, because γ_{eff} varies monotonically with T, while C is determined by the phase space at the Fermi surface, and hence is insensitive to T [9, 25, 26]. This produces a single peak when γ_{eff} is equal to the angular frequency ω of the applied compression oscillation (see (2.10)). As we will describe below, our results show that in the CFL phase, the situation is more complicated, because γ_{eff} is no longer a monotonic function of T, and also because C can vary rapidly as the control parameters δm and T are varied.

The dependence of the bulk viscosity (at frequency $\omega/2\pi = 1$ kHz) on the kaon energy gap δm is shown in the left panel of Fig. 6. From consideration of the factor of $\gamma_{\text{eff}}/(\gamma_{\text{eff}}^2 + \omega^2)$ in (2.10) we would have expected two peaks for $T = 0.01$ MeV and 0.1 MeV, because from Fig. 5 we see that at these temperatures γ_{eff} passes through $\omega = 1$ kHz at two different values of δm. In fact we get one peak, close to the lower value of δm at which $\gamma_{\text{eff}} = \omega$. The higher peak is washed out by rapid variation of C with δm, which occurs when $\delta m > T$ (see Fig. 4). Even outside the physically relevant range of δm shown in our plots, we do not find additional peaks in the bulk viscosity.

The dependence of the bulk viscosity (again at $\omega/2\pi = 1$ kHz) on the temperature T is shown in the right panel of Fig. 6. It is a monotonically increasing function of T for all values of δm. This is because, as is clear from the right panel of Fig. 4, C varies rapidly with temperature for all physically relevant values of δm. In fact, the temperature-dependence of C dominates the bulk viscosity, so the right panel of Fig. 6 looks similar to the right panel of Fig. 4.

Finally, Fig. 7 shows a plot of bulk viscosity ζ as a function of temperature for different oscillation timescales, $\tau = 2\pi/\omega$. We see that for unpaired quark matter,
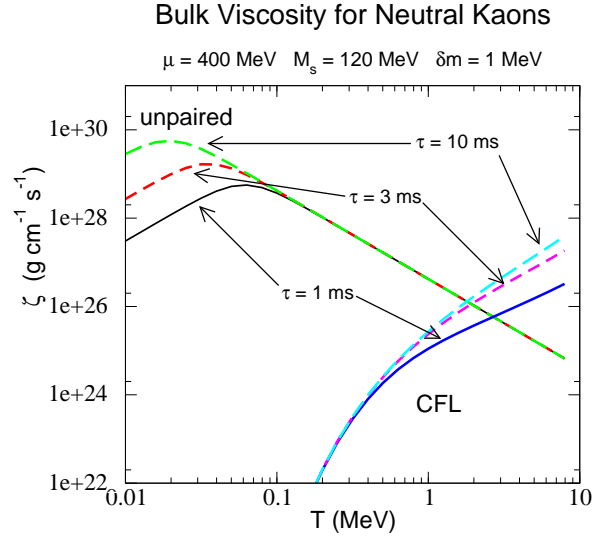
Figure 7: Bulk viscosity as a function of temperature for oscillations of different frequencies. The curves peaked on the left are for unpaired 3-flavor quark matter[9] and the rising curves on the right are our calculation of the kaonic bulk viscosity of CFL quark matter, for $\delta m = 1$ MeV.

ζ_{unp} is independent of ω at high temperatures, because γ_{unp} then rises far above ω, so, by (see (2.10)), $\zeta = C/\gamma_{\text{unp}}$. However, ζ_{CFL} depends more strongly on τ at high temperatures, because γ_{eff} is not much greater than ω at high temperature (Fig. 5), so the ω-dependence in (2.10) is not suppressed. The CFL bulk viscosity becomes larger as the frequency drops.

6   Conclusions

We have calculated the contribution of the lightest pseudo-Goldstone bosons, the neutral kaons, to the bulk viscosity of CFL quark matter. Our results are given by equations (2.10), (2.11), (4.2), (4.4), and are displayed for reasonable parameter choices in Figs. 6 and 7. The bulk viscosity is most sensitive to the temperature, and to the kaon energy gap δm (5.1). We find that, as one would expect, the kaonic bulk viscosity falls rapidly when the temperature drops below the kaon energy gap, since the the kaon population is then heavily Boltzmann-suppressed. It is clear from the right hand panel of Fig. 6 that once the temperature falls below the 10 MeV range (which is expected to occur in the first minutes after the supernova [27]) the bulk viscosity of CFL quark matter at kHz frequencies is suppressed by many orders of magnitude relative to that of unpaired quark matter.

It is noticeable that at low temperatures the suppression is less severe for smaller kaon energy gaps. However, δm is a poorly-known parameter of the effective theory of the pseudo-Goldstone bosons. It is the difference of the kaon mass and the kaon effective chemical potential, both of which are expected to be roughly of the order of 10 MeV [13], so it is unnatural to assume that δm is much smaller than an MeV or

so. For astrophysical applications, it is clear that CFL quark matter can be sharply distinguished from quark matter by its bulk viscosity (as by many other transport properties) after the very earliest times in the life of a compact star. Also, a rapidly vanishing bulk viscosity as the temperature drops below 10 MeV could be a potential observable associated with core collapse supernovae.

In general, bulk viscosity arises from re-equilibration in response to compression. We have calculated the dominant contribution to the re-equilibration of flavor in quark matter, and we believe that this is the dominant contribution to the bulk viscosity as a whole in the range of frequencies that are of astrophysical interest, namely zero to 1000 Hz. Any other contribution would have to come from degrees of freedom that equilibrate on a similar timescale, and the only possibility that we can imagine is the thermalization of the low-momentum tail of the thermal distribution of H particles.

Our results highlight several interesting questions for future research. A natural next step would be to extend our calculation to the kaon-condensed "CFL-K^0" phase, which corresponds to allowing the kaon energy gap to drop to zero. There are also some technical issues in our calculation of the flavor changing rate that remain to be addressed. The graph shown in Fig. 2 includes the width of the H boson due to the one-loop thermal self energy. This corresponds to the resummation of a class of diagrams with multiple H boson radiation and absorption [16]. However, since the mean free path associated with small angle two-body collisions is of the same order of magnitude as the radiation length (the mean free path between H-bremsstrahlung events) this approximation is not correct. A more complete approach has to take into account quantum mechanical inteference, the Landau-Pomeranchuk-Migdal (LPM) effect, between different diagrams that have the same final state [28]. Another relevant improvement would be to include higher-order corrections to the H dispersion relation [29] which could have a strong effect on the collinear splitting amplitude for H particles. We do not expect that these improvements will affect our results significantly, but they would change the numerical prefactors in the rate. Finally, it should be noted that we treated the kaon mass as a numerical parameter, but it is expected to be density-dependent, and its μ-dependence will feed into our expressions for the bulk viscosity. We expect that this would only weakly affect our results, but we have not performed an explicit check.

Acknowledgements

Appendix A Matching calculation of G_{ds} and v_{ds}

In this appendix we explain the matching calculation of the coefficients G_{ds} and v_{ds} in the effective lagrangian. As discussed in Sect. 3 these two coefficients can be extracted from the $B_\mu - X_\mu^6$ polarization function at zero energy and momentum transfer. The leading order contribution to the polarization function at very large baryon density is shown in Fig. 1. This two-loop diagram in can be viewed as the product of two one-loop polarization functions. This can be made more manifest by Fierz rearranging the weak interaction given in (3.22),

$$\mathcal{L} = -\frac{G_F V_{ud} V_{us}}{\sqrt{2}} (\bar{s}\gamma_\mu d)_L (\bar{u}\gamma^\mu u)_L. \tag{A.1}$$

We can now write the B_μ-X_μ^6 polarization function at $\omega = \vec{q} = 0$ as

$$\Pi_{\mu\nu}^{XB} = -\frac{G_F V_{ud} V_{us}}{\sqrt{2}} \Pi_{\mu\alpha}^{(sd)_L} \Pi_{\alpha\nu}^{(uu)_L}, \tag{A.2}$$

where $\Pi_{\mu\nu}^{(sd)_L}$ and $\Pi_{\mu\nu}^{(uu)_L}$ are the polarization functions of the currents $(\bar{s}\gamma_\mu d)_L$ and $(\bar{u}\gamma^\mu u)_L$ in the limit of vanishing energy and momentum transfer. The polarization functions have the tensor decomposition

$$\Pi_{\mu\nu} = f^2 \left(\delta_{\mu 0}\delta_{\nu 0} - v^2 \delta_{\mu i}\delta_{\nu i} \right), \tag{A.3}$$

where f and v can be viewed as the decay constant and velocity of a collective mode. The relevant correlation functions in the CFL phase were first computed by Son and Stephanov [19]. Using their results we can write

$$\Pi_{\mu\nu}^{XB} = -\frac{G_F V_{ud} V_{us}}{\sqrt{2}} 2 f_\pi^2 f_H^2 \left(\delta_{\mu 0}\delta_{\nu 0} - v^4 \delta_{\mu i}\delta_{\nu i} \right), \tag{A.4}$$

where f_π and f_H are the pion and H decay constants, see equ. (3.12),(3.20), and v is the Goldstone boson velocity. Comparing with (3.24) we conclude that

$$G_{ds} = -\sqrt{2} G_F V_{ud} V_{us}, \qquad v_{ds}^2 = v^2 = 1/3. \tag{A.5}$$

References

[1] K. Rajagopal and F. Wilczek, hep-ph/0011333. M. G. Alford, Ann. Rev. Nucl. Part. Sci. **51** (2001) 131 [hep-ph/0102047]. D. K. Hong, Acta Phys. Polon. B **32**, 1253 (2001) [hep-ph/0101025]. D. H. Rischke, Prog. Part. Nucl. Phys. **52**, 197 (2004) [nucl-th/0305030]. T. Schäfer, hep-ph/0304281. S. Reddy, Acta Phys. Polon. B **33**, 4101 (2002) [arXiv:nucl-th/0211045].

[2] M. Alford, K. Rajagopal and F. Wilczek, Nucl. Phys. **B537**, 443 (1999) [hep-ph/9804403].

[3] F. Weber, Prog. Part. Nucl. Phys. **54**, 193 (2005) [arXiv:astro-ph/0407155].

[4] J. M. Lattimer and M. Prakash, Astrophys. J. **550**, 426 (2001) [astro-ph/0002232];

[5] J. L. Friedman and K. H. Lockitch, gr-qc/0102114.

[6] N. Andersson, Class. Quant. Grav. **20**, R105 (2003) [arXiv:astro-ph/0211057].

[7] K. D. Kokkotas and N. Andersson, arXiv:gr-qc/0109054.

[8] J. Madsen, Phys. Rev. Lett. **85**, 10 (2000) [arXiv:astro-ph/9912418].

[9] J. Madsen, Phys. Rev. D **46**, 3290 (1992).

[10] Q. D. Wang and T. Lu, Phys. Lett. B **148**, 211 (1984).

[11] P. F. Bedaque and T. Schäfer, Nucl. Phys. A **697** (2002) 802 [hep-ph/0105150].

[12] D. B. Kaplan and S. Reddy, Phys. Rev. D **65**, 054042 (2002) [arXiv:hep-ph/0107265].

[13] T. Schäfer, Phys. Rev. D **65**, 094033 (2002) [arXiv:hep-ph/0201189].

[14] M. Alford and K. Rajagopal, JHEP **0206**, 031 (2002) [arXiv:hep-ph/0204001].

[15] D. T. Son, arXiv:hep-ph/0204199.

[16] C. Manuel, A. Dobado and F. J. Llanes-Estrada, JHEP **0509**, 076 (2005) [arXiv:hep-ph/0406058].

[17] C. Manuel, PoS **JHW2005**, 011 (2006) [arXiv:hep-ph/0512054].

[18] R. Casalbuoni and R. Gatto, Phys. Lett. B **469**, 213 (1999) [arXiv:hep-ph/9909419].

[19] D. T. Son and M. A. Stephanov, Phys. Rev. D **61**, 074012 (2000) [arXiv:hep-ph/9910491]; Erratum: Phys. Rev. D **62**, 059902 (2000) [arXiv:hep-ph/0004095].

[20] T. Schäfer, Nucl. Phys. B **575**, 269 (2000) [arXiv:hep-ph/9909574].

[21] C. Manuel and M. H. G. Tytgat, Phys. Lett. B **479**, 190 (2000) [arXiv:hep-ph/0001095].

[22] J. F. Donoghue, E. Golowich and B. R. Holstein, Camb. Monogr. Part. Phys. Nucl. Phys. Cosmol. **2**, 1 (1992).

[23] P. Jaikumar, M. Prakash and T. Schäfer, Phys. Rev. D **66**, 063003 (2002) [arXiv:astro-ph/0203088.

[24] S. Reddy, M. Sadzikowski and M. Tachibana, Phys. Rev. D **68**, 053010 (2003) [arXiv:nucl-th/0306015.

[25] B. A. Sa'd, I. A. Shovkovy and D. H. Rischke, arXiv:astro-ph/0607643.

[26] M. G. Alford and A. Schmitt, J. Phys. G: Nucl. Part. Phys. **34** 67 (2007) [arXiv:nucl-th/0608019].

[27] A. Burrows and J. M. Lattimer, Astrophys. J. **307**, 178 (1986).

[28] P. Arnold, G. D. Moore and L. G. Yaffe, JHEP **0301**, 030 (2003) [arXiv:hep-ph/0209353].

[29] K. Zarembo, Phys. Rev. D **62**, 054003 (2000) [arXiv:hep-ph/0002123].